Original Paper

Cellular Physiology and Biochemistry

Cell Physiol Biochem 2011;28:613-624

Accepted: October 28, 2011

TASK-1 Channels May Modulate Action Potential Duration of Human Atrial Cardiomyocytes

Sven H. Limberg[1,2,†], Michael F. Netter[1,†], Caroline Rolfes[2,†], Susanne Rinné[1,†], Günter Schlichthörl[3], Marylou Zuzarte[3], Timon Vassiliou[2], Rainer Moosdorf[4], Hinnerk Wulf[2], Jürgen Daut[3], Frank B. Sachse[5] and Niels Decher[1]

[1]Institut für Physiologie und Pathophysiologie, Abteilung vegetative Physiologie, Universität Marburg, Marburg, [2]Klinik für Anästhesiologie und Intensivtherapie, Universitätsklinikum Giessen und Marburg, Standort Marburg, [3]Institut für Physiologie und Pathophysiologie, Abteilung Zellphysiologie, Universität Marburg, Marburg, [4]Klinik für Herz- und thorakale Gefäßchirurgie, Universitätsklinikum Giessen und Marburg, Standort Marburg, [5]Bioengineering Department and the Nora Eccles Harrison Cardiovascular Research and Training Institute, University of Utah, Salt Lake City, [†]These authors contributed equally to this work

Key Words

Cardiac potassium current • Ion channel modulation • Potassium channel • Human atrial auricles • A293

Abstract

Background/Aims: Atrial fibrillation is the most common arrhythmia in the elderly, and potassium channels with atrium-specific expression have been discussed as targets to treat atrial fibrillation. Our aim was to characterize TASK-1 channels in human heart and to functionally describe the role of the atrial whole cell current I_{TASK-1}. Methods and Results: Using quantitative PCR, we show that TASK-1 is predominantly expressed in the atria, auricles and atrio-ventricular node of the human heart. Single channel recordings show the functional expression of TASK-1 in right human auricles. In addition, we describe for the first time the whole cell current carried by TASK-1 channels (I_{TASK-1}) in human atrial tissue. We show that I_{TASK-1} contributes to the sustained outward current I_{Ksus} and that I_{TASK-1} is a major component of the background conductance in human atrial cardiomyocytes. Using patch clamp recordings and mathematical modeling of action potentials, we demonstrate that modulation of I_{TASK-1} can alter human atrial action potential duration. Conclusion: Due to the lack of ventricular expression and the ability to alter human atrial action potential duration, TASK-1 might be a drug target for the treatment of atrial fibrillation.

Copyright © 2011 S. Karger AG, Basel

Introduction

Atrial fibrillation (AF) is a major risk factor for morbidity and mortality in the elderly. Mortality in AF is primarily caused by heart failure and thromboembolic complications [1]. Current therapeutic concepts include the control of ventricular heart rate, restoration of sinus rhythm and prevention of recurrence of AF. However, therapeutic efficiency is limited due to electrical and structural remodeling caused by AF [2]. Slowing of atrial repolarization by blocking K^+ channels can terminate AF by prolonging the effective refractory period. However, most antiarrhythmic drugs currently available also

KARGER

Fax +41 61 306 12 34
E-Mail karger@karger.ch
www.karger.com

© 2011 S. Karger AG, Basel
1015-8987/11/0284-0613$38.00/0

Accessible online at:
www.karger.com/cpb

Niels Decher
Institut für Physiologie, Vegetative Physiologie, Universität Marburg
Deutschhausstraße 1-2, 35037 Marburg (Germany)
Tel. +49 6421 28 62148, Fax +49 6421 28 66659
E-Mail decher@staff.uni-marburg.de

prolong the ventricular action potential which increases the risk of *torsades de pointes* arrhythmias and sudden cardiac death due to ventricular fibrillation. These severe adverse effects can be avoided by blocking atrial-specific potassium currents. Specific potassium channel targets of the atrium suggested so far include channels underlying the ultra-rapid delayed rectifier current I_{Kur} and the acetylcholine-activated current I_{KAch} [3]. It has been speculated that two-pore domain potassium channels contribute to native cardiac K^+ currents [4, 5]. Due to a lack of specific TASK-1 blockers, it was in the past not possible to isolate native atrial I_{TASK-1} in human heart. We have recently used the TASK-1 specific blocker A293 to isolate I_{TASK-1} in rat and mouse ventricular cardiomyocytes [6, 7]. In the present study we show that in the human heart TASK-1 is specifically expressed in the atrium and we provide a quantitative description of I_{TASK-1} in human atrial myocytes. We show that I_{TASK-1} might modulate action potential duration using whole cell and dynamic patch clamp experiments in human atrial cells. In addition, mathematical modeling of the atrial action potential supports the role of TASK-1 in the repolarization phase. Our results suggest that TASK-1 has an atrium-specific expression in the human heart and that I_{TASK-1} might influence atrial action potential duration. Thus, TASK-1 might be a promising drug target for the treatment or prevention of AF.

Materials and Methods

Ethical approval

The investigation conforms to the principles outlined in the Declaration of Helsinki and to the guide for the Care and Use of laboratory Animals (NIH Publication 85-23). The study was approved by the local ethics committee of the Marburg University (medical faculty) (No. 53/07). Each patient gave written informed consent.

Isolation of human atrial cardiomyocytes

Right atrial auricle specimens were obtained from 12 patients with sinus rhythm undergoing cardiac surgery in extracorporeal circulation. The preparation of human auricle cardiomyocytes was previously described [8-9] and modified only marginally. Briefly, after biopsy specimens were stored for 60 min at 4 °C in calcium-free solution containing in mM: NaCl 27, KCl 20, $MgCl_2$ 1.5, HEPES 5, Glucose 274; pH 7.0. Then, specimens were cut into pieces of 1-2 mm^3 and oxygenized (tension: 100-150 mmHg) at 37 °C in 10 ml of calcium-free solution containing in mM: NaCl 140, KCl 5.4, $MgCl_2$ 1.2, HEPES 5, Glucose 5; pH 7.0. Using a miniature magnetic stirring bar rotating with 3 Hz, blood and calcium was washed out of the specimens three times for 7 min each. Specimens were then transferred into calcium-free solution containing 720 U/ml collagenase Type 2 (Worthington), 0.52 U/ml protease Type XXIV (Sigma) and 0.1 % bovine albumin. After 30 min of digestion, cells in suspension were separated from debris by centrifuging at 2000 rpm for 2 min. Rod-shaped striated cells were then placed on 35 mm dishes for measurements.

Expression analysis

Total RNA from human hearts of 12 patients with sinus rhythm (Table 1) was isolated using a RNA/DNA/Protein Purification Kit (Norgen). Reverse transcription (RT) was performed with random hexamer primers (Applied Biosystems) and Superscript II reverse transcriptase (Invitrogen) according to the instructions of the manufacturer. Subsequently cDNA was pooled. Multiple cardiac tissues were analyzed with a commercial cardiac tissue cDNA panel (Clontech). PCRs were performed with intron-spanning primers using the Platinum SYBR Green qPCR SuperMix-UDG (Invitrogen) according to the instructions of the manufacturer. Reaction mixtures were preheated at 50 °C for 2 min and at 95 °C for 2 min, followed by 40 cycles at 95 °C for 15 s, 60 °C for 30 s, and 72 °C for 30 s. Emitted fluorescence was detected online using a Mx3000P real-time PCR system (Stratagene). For all primer pairs the amplification products were confirmed by sequencing, no template control (NTC) and dissociation curve analysis. In addition, amplification efficiency was determined by analyzing the slope of a CT/log (template concentration) plot. For normalization, primers for glyceraldehyde-3-phosphate dehydrogenase (GAPDH) were used ($rE=1/2^{\Delta CT}$). Primers used in quantitative RT-PCR expression analysis: GAPDH for 5'-AGT CAA CGG ATT TGG TCG TAT-3', rev 5'-ACC ATG TAG TTG AGG TCA ATG AAG-3'; Kv1.5 for 5'-CCC TGG AGA ATG CAG ACA GT-3', rev 5'-TCC AGG CAG AGG GCA TAA AG-3'; Kv2.1 for 5'-TAC TGG AGA AGC CCA ATT CCT CTG-3', rev 5'-CTG TAG CTC AGG CAG CGT GTT G-3'; Kv4.3long for 5'-CTT GTG GAT GAT CCC CTG TTA TCT-3', rev 5'-GGT AGT TCT GCA TTG AAC TCT CCA-3'; Kir2.1 for 5'-CAG TTC ATC AAT GTG GGT GAG AAG-3', rev 5'-ACG AAA GCC AGG CAG AAG ATA AC-3'; KCNQ1 for 5'-TGG AGA GAA GAT GCT CAC AGT CC-3', rev 5'-TGT TGG GCT CTT CCT TAC AGA ACT-3'; hERG for 5'-CAT TGT GGA CAT CCT CAT CAA CTT-3', rev 5'-GAG GAA CCA GCC CTT GAA GTA GT-3'; TREK-1b for 5'-GAA TGC TGC ATG CCT CAT GCT T-3', rev 5'-AAT GAG AGC CTC GGT TTG GAG TTC-3'; TASK-1 for 5'-TTC GCC GGC TCC TTC TAC TTC-3', rev 5'-CGT AGA ACA TGC AGA ACA CCT TG-3'.

Expression of TASK-1 channels in Xenopus oocytes

Xenopus oocytes were prepared as previously described [10]. Isolated oocytes were stored at 18 °C in ND96 recording solution containing in mM: NaCl 96, KCl 2, $CaCl_2$ 1.8, $MgCl_2$ 1, HEPES 5; pH 7.4 with NaOH, supplemented with Na-pyruvate (275 mg/l), theophylline (90 mg/l) and gentamicin (50 mg/l). Stage IV and V oocytes were injected with 1.5 ng of TASK-1 cRNA, synthesized using the mMESSAGE mMACHINE Kit (Ambion). Standard two-electrode voltage-clamp (TEVC) experiments were performed at room temperature (21 - 22 °C) in ND96 recording solution 2 days after injection. Microelectrodes were fabricated from glass capillary tubes and filled with 3 M

KCl. Tip resistance was in the range of 0.2-1.0 MΩ. Two-electrode-voltage clamp (TEVC) recordings were performed using a TurboTEC-10CD Amplifier (npi) with a Digidata 1200 A/D-converter (Axon Instruments). For data acquisition the software pCLAMP7 (Axon Instruments) was used and data were analyzed with ClampFit10 (Axon Instruments).

Patch clamp

Isolated cardiomyocytes were placed on 35 mm dishes (Corning). After 15 minutes of settling, patch clamp recordings were performed at room temperature (21 - 22 °C). Pipettes had a tip resistance of 2.0 - 3.5 MΩ when filled with the pipette solution containing in mM: KCl 60, K-glutamate 65, EGTA 5, $MgCl_2$ 2, K_2ATP 3, Na_2GTP 0.2 and HEPES 5; pH 7.2 with KOH. Cells were perfused with a bath solution containing in mM: NaCl 140, KCl 5.4, $CaCl_2$ 1, $MgCl_2$ 1, NaH_2PO_4 0.33, glucose 10 and HEPES 5; pH 7.4 with NaOH. Series resistances were automatically compensated by 70 %. For single channel measurements we used a pipette solution which was free of divalent cations, containing in mM: 140 KCl, 5 HEPES; pH 7.2 with KOH.

Dynamic patch clamp

Dynamic patch clamp recordings were performed utilizing a custom written software based on LabView (National Instruments). An Axopatch 200B amplifier (Axon Instruments) was controlled by a 16 bit adc/dac card from National Instruments. The current injected was calculated from the input potential by the GHK current equation. According to the action potential frequency, an additional depolarization pulse was applied (see also Fig. 3). Sequences of 20 action potentials were recorded and the duration of the last 10 action potentials was evaluated. The sampling rate was 570 Hz.

Drugs

*A*293 (2-(Butane-1-sulfonylamino)-N-[1-(R)-(6-methoxy-pyridin-3-yl)-propyl]-benzamide) was obtained from Sanofi Aventis GmbH Germany. When high concentrations of A293 were used, TASK-1 currents were recorded in a blocker mixture solution in order to avoid side effects of A293 on other ionic currents, as previously described [6]. The blocker mixture contained in μM: E-4031 1, HMR-1556 2, 4-AP 2000, glibenclamide 2, nifedipine 10. Drugs were stored as DMSO stocks and final DMSO concentration did not exceed 0.1 %.

Data analysis

Results are reported as mean ± S.E.M. (n = number of cells). Statistical differences were evaluated using unpaired Student's t-tests, unless stated otherwise. Significance was assumed for $p < 0.05$, as indicated by an asterisk (*) or $p < 0.01$, as indicated by two asterisks (**).

TASK-1 Markov model and action potential modeling

A Markov model of TASK-1 channels was developed using Matlab software (MathWorks Inc). The model included two closed states, C1 and C2, and an open state O (Fig. 4I, top). Forward rate α and backward rate β were defined as dependent on the membrane voltage V_m:

		Patients n = 12
Gender	male	11 (92 %)
	female	1 (8 %)
Age	≤ 60	2 (17 %)
	61-75	10 (83 %)
	≥ 76	0 (0 %)
LV-function	normal	12 (100 %)
	moderate-to-serve dysfunction	0 (0 %)
Pharmacological treatment	ACE-inhibitor	7 (58 %)
	β-blocker	7 (58 %)
	Ca^{2+}-antagonist	3 (25 %)
	digitoxin	1 (8 %)
	loop-diuretic	6 (50 %)
	K^+-sparing diuretic	3 (25 %)
	thiazide-diuretic	2 (17 %)
	statin	6 (50 %)
	glyceryl trinitrate	1 (8 %)
Cardiosurgical procedure	coronary artery bypass	8 (67 %)
	aortic valve replacement	3 (25 %)
	mitral valve replacement or repair	1 (8 %)
	thoracic aneurysm repair	1 (8 %)
	left ventricular aneurysmectomy	1 (8 %)

Table 1. Characteristics of patients with sinus-rhythm pooled for qPCR experiments.

$$\alpha = \alpha_0 e^{z_\alpha \frac{V_m F}{RT}} \qquad \beta = \beta_0 e^{-z_\beta \frac{V_m F}{RT}}$$

with the rates α_0 and β_0 at 0 mV, the charges z_α and z_β, the temperature T, Faraday constant F, and the gas constant R. I_{TASK-1} was described by the Goldman-Hodgkin-Katz equation for potassium currents as described previously [6, 11]. Parameters of the Markov model were determined using a previously developed stochastic approach for numerical fitting [12] applied to the data recorded using the two electrode voltage clamp technique.

A mathematical model of human atrial myocytes [13] was used to simulate effects of I_{TASK-1} on action potentials. The potassium permeability P_{TASK-1} was adjusted to reproduce the patch clamp experiments with isolated human cardiomyocytes. Cells were stimulated at a rate of 1 Hz. The simulations with the myocyte model were carried out with the Euler method for numerical solution of ordinary differential equations [14]. Simulation results after the 10th stimulation were analyzed.

Results

Expression of TASK-1 in the human heart

As a first step in characterizing the role of TASK-1 in human heart, we analyzed the expression level and expression pattern in different cardiac tissues. A cDNA pool of human atrial auricles from 12 patients not suffering

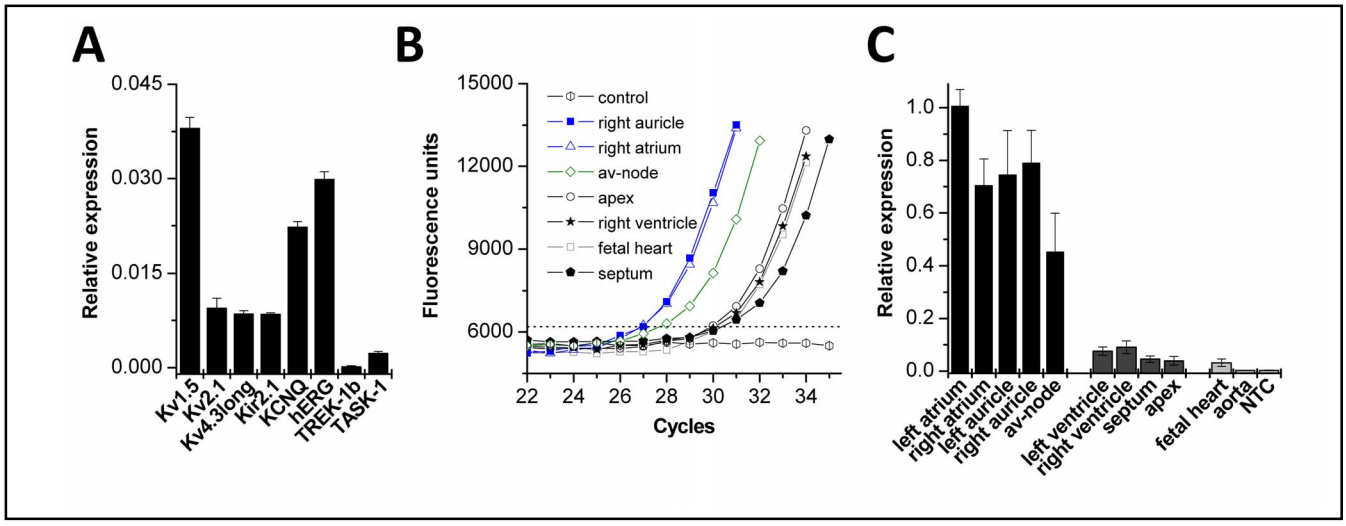

Fig. 1. Expression analysis of TASK-1 in the human heart. (A), Quantitative mRNA expression analysis of human TASK-1 in heart tissue pooled from 12 different donors (n = 8 qPCR runs). Relative expression was quantified as $1/2^{\Delta CT}$, where ΔCT is CT (GAPDH) - CT (K^+ channel). (B), Sample amplification blots of quantitative PCR analysis of human TASK-1 in different cardiac tissues. (C), Quantitative PCR data analyzing the TASK-1 expression in various cardiac regions, normalized to left atrium (n = 5 qPCR runs). For patient information see Table 1 or Material and Methods section.

from AF (Table 1) was prepared and analyzed by quantitative PCR experiments. First, we analyzed the relative expression of the most prominent cardiac potassium channels including the K_{2P} channels TREK-1 and TASK-1 (Fig. 1A). The quantitative PCR experiments showed that TASK-1 had an mRNA expression level which was about three times lower than that of the I_{K1} and I_{to} components Kir2.1 and Kv4.3. Next, we analyzed the relative expression of TASK-1 in different cardiac regions (Fig. 1B, C). For this purpose, commercial cDNA pools (Clontech) of different regions of human heart were analyzed. Interestingly, expression of TASK-1 was restricted to the atria including auricles and the atrio-ventricular node (Fig. 1C). In contrast, no or only low mRNA expression levels were observed in the ventricles, the interventricular septum, the apex of the heart, the aorta and the fetal heart (Fig. 1C).

Electrophysiological characterization of TASK-1 currents in human atrial cells

After characterizing expression of TASK-1 at the mRNA level, we aimed to record TASK-1 single channel currents in right auricular myocytes to prove the functional expression in human atria. The characteristics of the patients examined in our patch clamp studies are listed in Table 2. An example of a cell attached recording with a TASK-1 like channel in a divalent cation-free solution is depicted in Fig. 2A. The TASK-1 like channel in human atrial auricles had a slope conductance of 28 ± 1 pS (n = 4), calculated in the voltage range of -50 to -110 mV. The open probability was determined using long voltages steps with a duration of 60 s (n = 4) to potentials in the range of -50 to -110 mV. For all tested potentials the open probability was low, with $p < 0.01$ (n = 4). A magnification of the brief openings on an expanded

		Patients n = 6
Gender	male	2 (33 %)
	female	4 (67 %)
Age	≤ 60	0 (0 %)
	61-75	6 (100 %)
	≥ 76	0 (0 %)
LV-function	normal	5 (83 %)
	moderate-to-serve dysfunction	1 (17 %)
Pharmacological treatment	ACE-inhibitor	4 (67 %)
	β-blocker	3 (50 %)
	Ca^{2+}-antagonist	1 (17 %)
	digitoxin	0 (0 %)
	loop-diuretic	3 (50 %)
	K^+-sparing diuretic	2 (33 %)
	thiazide-diuretic	2 (33 %)
	statin	3 (50 %)
	glyceryl trinitrate	2 (33%)
Cardiosurgical procedure	coronary artery bypass	3 (50 %)
	aortic valve replacement	3 (50 %)
	thoracic ancurysm repair	1 (17 %)

Table 2. Characteristics of patients examined in the patch-clamp experiments.

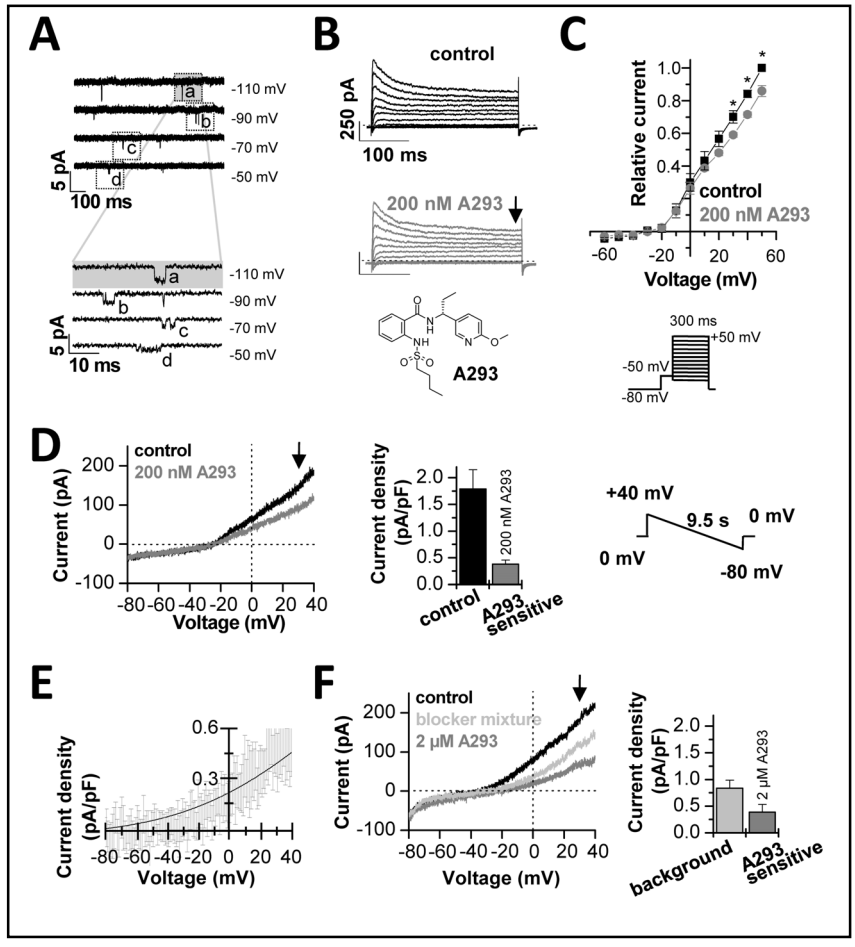

Fig. 2. Electrophysiological characterization of human cardiac I_{TASK-1}. (A), Cell attached recordings from a TASK-1 like channel in human atrial cardiomyocytes. The lower panel shows a magnification of the events designated in the top panel by dotted squares. (B), Representative current traces elicited by the voltage protocol illustrated in panel C. After a pre-step of 70 ms to -50 mV, the voltage was stepped for 300 ms from -60 mV to +50 mV in 10 mV increments. The holding potential was -80 mV and the sweep time interval was 10 s. Control traces are shown in black and traces after administration of 200 nM A293 in grey. The chemical structure of A293 is illustrated below. (C), Mean current voltage relationships in the absence and presence of A293 derived at the end of the 300 ms test pulse (as indicated by the arrow in panel B). Significance was analyzed using a paired Student´s t-test. (D), Isolation of the A293-sensitive TASK-1 current, using 200 nM A293. Currents were recorded using the shown voltage ramps from +40 mV to -80 mV (duration 9.5 s) from a holding potential of 0 mV. Control traces are shown in black. The bar graph in the middle panel analyzes the currents measured at +30 mV (as illustrated by the arrow) and the difference current analyzed after application of the TASK blocker A293 (which corresponds to I_{TASK-1}). (E), Depicted is the average difference current with S.E.M., isolated with 200 nM A293 (n = 7). The solid line indicates a fit to the GHK equation. (F), Recordings of a background conductance after application of a blocker mixture (light grey), using the same protocols and analysis as described above. 2 µM A293 (in the presence of the blocker mixture) was used to isolate the A293-sensitive TASK-1 currents and the relative contribution to the background current.

time scale is shown in the lower panel of Fig. 2A. The mean open time of the TASK-1 like channel was 0.99 ± 0.03 ms (n = 4). These data on single channel kinetics of the TASK-1 like channel in human atria are in good agreement with TASK-1 channels recorded in divalent cation-free solutions [15] or in rat cardiomyocytes [6, 16].

Our next aim was to quantify the macroscopic whole cell current carried by atrial TASK-1 channels (Fig. 2B-F) using the TASK-1 blocker A293, which we have previously characterized [6]. The inset of Fig. 2B illustrates the chemical structure of the blocker. At a concentration of 200 nM, A293 causes an almost complete inhibition of TASK-1 [6]. At this concentration A293 has virtually no effect on other cardiac channels [6]. Representative current voltage relationships of right human auricular cardiomyocytes recorded before and after application of A293 are illustrated in Fig. 2B and C. In these experiments the sustained outward current I_{Ksus} was analyzed at the end of a 300 ms test pulse. The I_{Ksus} had a current density of 3.88 ± 0.74 pA/pF (n = 5) at +30 mV, similar as previously described [17]. After application of 200 nM A293, the sustained outward current analyzed at +30 mV, was blocked by 15.0 ± 2.9 % (n = 5) (Fig. 2C).

In order to improve isolation of the I_{TASK-1} current, we subsequently used voltage ramp protocols (Fig. 2D-F) and a blocker mixture (Fig. 2F) that were optimized for this purpose [6]. In addition, the holding potential between the voltage ramps was set to 0 mV, to further suppress inactivating currents. A representative voltage ramp recording from human atrial cardiomyocytes before and after application of A293 is shown in Fig. 2D (left panel). I_{TASK-1} isolated with 200 nM A293 was 0.38 ± 0.08 pA/pF (n = 7) at +30 mV (Fig. 2D, middle panel). Figure 2E illustrates the average difference

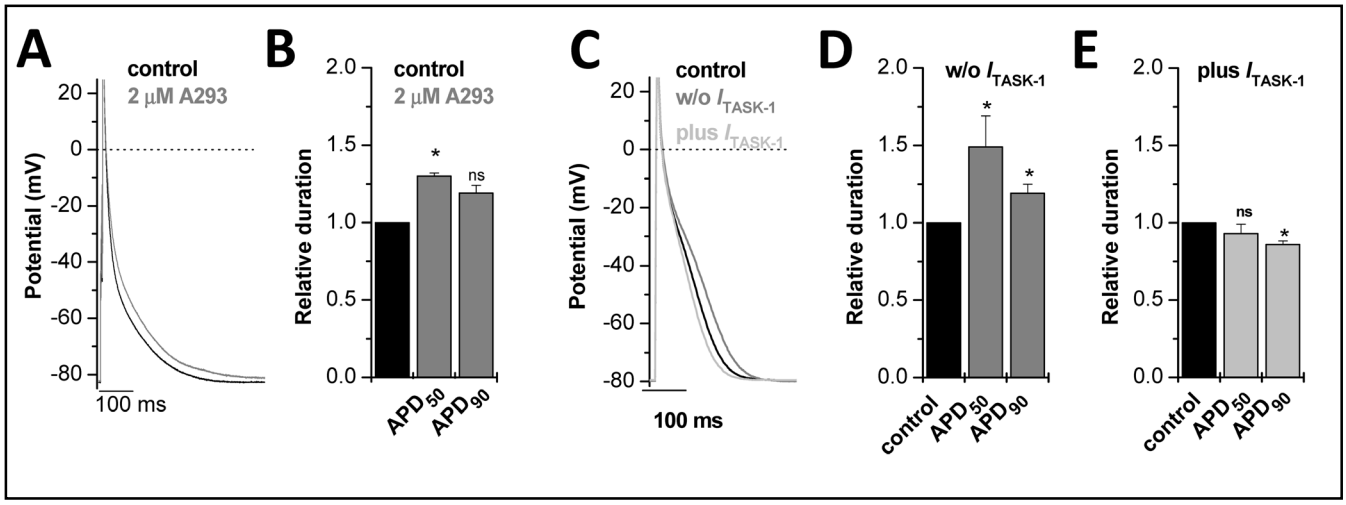

Fig. 3. Patch clamp recordings of right human auricle cardiomyocytes. (A), Right auricle cardiomyocytes were injected with a small negative current of about -20 pA in order to hyperpolarize the cells to -80 mV. Action potentials were elicited by injection of a 2 - 5 ms current pulse of 2 nA amplitude. Action potentials were evoked with a frequency of 1 Hz. After action potential duration reached a steady state (black), 2 μM A293 was administered, until steady-state was reached (grey). (B), Relative increase in APD_{50} and APD_{90} by 2 μM A293. (C), Dynamic patch clamp experiments of single myocytes were performed as previously described [37]. Right human auricle cardiomyocytes were held in current clamp mode and resting membrane potential was adjusted to -80 mV via the injection of a negative offset current, as described above. Action potentials were elicited at a frequency of 1 Hz via injection of a positive current pulse (2 - 3 nA) of 2 ms duration. Dynamic patch clamp experiments with subtraction of I_{TASK-1} led to prolonged action potential (dark grey line), injection of an additional I_{TASK-1} shortened APD (light grey line). (D), Bar graph showing prolongation of APD_{50} and APD_{90}, respectively after subtraction of I_{TASK-1}. (E), Shortening of APD_{50} and APD_{90} after injecting additional I_{TASK-1}.

current with S.E.M., isolated with 200 nM A293 (n = 7). The rectification of the difference current is in good agreement with a K_{2P} channel that obeys the GHK equation (illustrated as solid line) (Fig. 2E).

Next, we aimed to analyze the relative contribution of I_{TASK-1} to the background conductance of human atrial cardiomyocytes. Therefore, we used a blocker mixture [6] to pharmacologically suppress any remaining contributions of I_{KATP}, I_{to}, I_{Ca}, I_{Kr} and I_{Ks} to the cardiac background current (Fig. 2F, trace in light grey). In the presence of the blocker mixture the background current density was 0.84 ± 0.15 pA/pF (n = 9) (Fig. 2F, right panel). In addition, we applied high concentrations (2 μM) of A293 to ensure a complete inhibition of TASK-1 channels. In the presence of the blocker mixture, application of 2 μM A293 resulted in a strong inhibition of the background conductance (Fig. 2F, trace in dark grey). The I_{TASK-1} current isolated in this way was 0.39 ± 0.14 pA/pF at +30 mV (n = 9) (Fig. 2F, right panel). These measurements suggest that I_{TASK-1} contributes about 40 % to the background current of native human atrial cardiomyocytes.

Combining both sets of data obtained with slow voltage ramp protocols from 0 mV gave an average I_{TASK-1} density of 0.38 pA/pF at +30 mV. The mean amplitude of I_{TASK-1} from both sets of experiments (Fig. 2D, F) was 34 pA at +30 mV and the mean membrane capacity was 94 pF.

I_{TASK-1} currents modulate human atrial action potential duration

Next, we tested whether I_{TASK-1} currents are important for the repolarization of human atrial action potentials. For these experiments, cells were held at -80 mV in the current clamp modus before injection of brief depolarizing pulse at a frequency of 1 Hz. In addition, we used 2 μM of A293 to ensure a complete inhibition of TASK-1 channels. Application of A293 led to a prolongation of action potential duration (Fig. 3A, grey trace). APD_{50} and APD_{90} (Fig. 3B) were prolonged from 18.2 ± 3.5 ms to 23.0 ± 4.8 ms (+30 %, n = 3) and from 141.6 ± 6.1 ms to 167.55 ± 0.3 ms (+19 %, n = 3), respectively.

As a control experiment, we addressed the question whether a current of ~0.38 pA/pF can modulate the action potential duration of human atrial cardiomyocytes, using dynamic patch clamp recordings. For dynamic patch clamp recordings the action potentials were elicited with

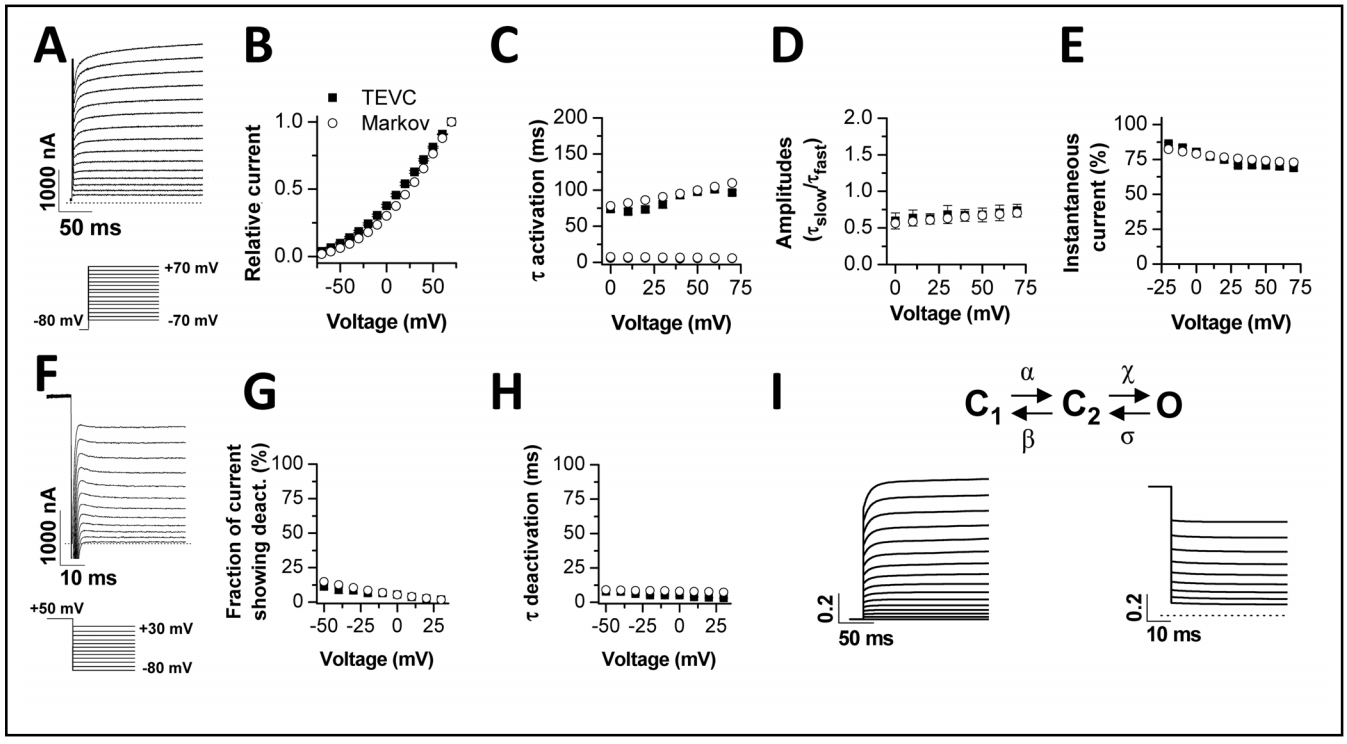

Fig. 4. Development of a TASK-1 Markov model. TEVC measurements of TASK-1 channels in *Xenopus* oocytes served to create a Markov model based on a closed-closed-open assumption. The figure illustrates the comparison of biophysical parameters of TASK-1 injected oocytes measured by TEVC (squares) and the Markov model (circles). (A), Representative TASK-1 current voltage relationship recordings elicited by the voltage protocol illustrated. The recordings in (A) served as input for the comparison of TASK-1 model data with TEVC recordings (B-E). (B), Current voltage relationship. (C), Time constants of activation. (D), Ratio of the amplitudes of the time constants of activation. (E), Percentage of instantaneous current. (F), Representative recordings of TASK-1 deactivation, using the illustrated voltage protocol. The recordings in (F) served as input for the comparison to the TASK-1 model data (G-H). (G), Fraction of current showing deactivation. (H), Time constant of deactivation. (I), Scheme of the Markov model with simulated currents for activation (left) and deactivation (right). Currents were normalized.

a short current pulse, similar as for the action potential recordings described above. During the subsequent action potential I_{TASK-1} was subtracted or added (Fig. 3C). The Goldman-Hodgkin-Katz current equation was used to determine the amount of current that had to be injected at any given potential during the action potential. The calculations were performed with $[K^+]_i$ of 150 mM, $[K^+]_o$ of 5 mM and an I_{TASK-1} amplitude of 30 pA at +30 mV. The shape and duration of the action potentials recorded under control conditions was similar as previously described (Fig. 3C) [18]. The APD_{50} was 31.2 ± 8.9 ms and the APD_{90} was 147 ± 20 ms (n = 10). The subtraction of I_{TASK-1} (mimicking a block of the channel) prolonged the APD_{50} significantly to 56.5 ± 22.7 ms (+49 %, n = 10) and the APD_{90} to 183 ± 35 ms (+19 %, n = 10) (Fig. 3D). Previously, it has been shown that TASK-1 transcription is about 2-fold up-regulated in atrial fibrillation [19]. Injection of I_{TASK-1} (mimicking a doubling of native I_{TASK-1}) led to a significant shortening of the APD_{90} to 124 ± 15 ms (-16 %, n = 10), while the APD_{50} was not significantly affected (25.8 ± 6.3 ms, n = 10) (Fig. 3E). We therefore conclude that up-regulation

Name	Symbol	Value	Unit
Rate constant for C1 - C2	α_0	13.3	s^{-1}
Charge for C1 - C2	z_α	-0.106	
Rate constant for C2 - C1	β_0	17.6	s^{-1}
Charge for C2 - C1	Z_β	-0.105	
Rate constant for C2 - O	χ_0	108	s^{-1}
Charge for C2 - O	z_χ	0.095	
Rate constant for O - C2	δ_0	9.7	s^{-1}
Charge for O - C2	z_δ	0.307	

Table 3. Parameters for rate coefficients of Markov model of I_{TASK-1}. For usage of the parameters see also Fig. 4I and the equations in the Material and Methods section.

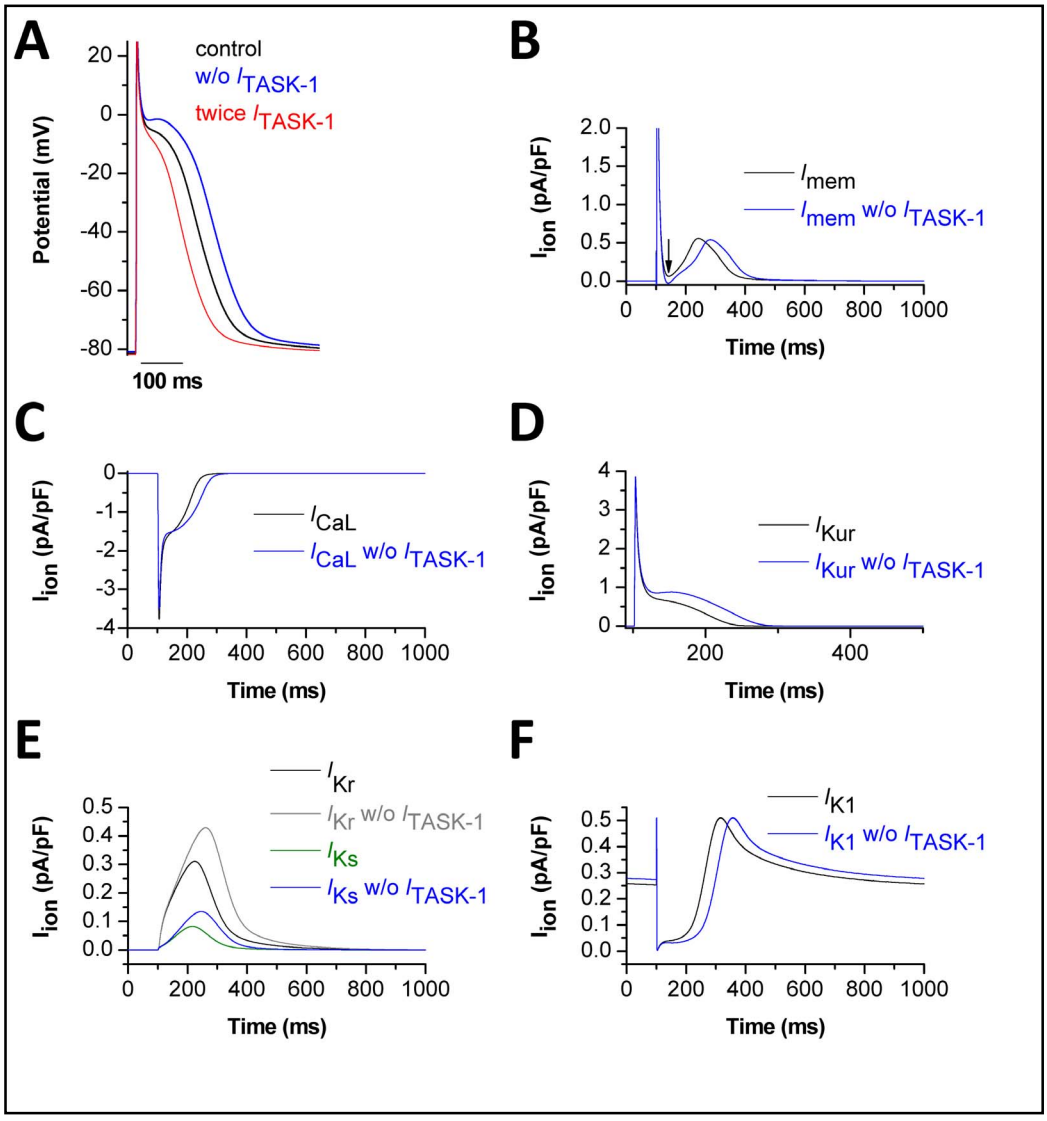

Fig. 5. Action potential simulations using the TASK-1 Markov model show the influence of I_{TASK-1} on human atrial action potential. (A), Computational simulation of a normal action potential (black). Subtraction of I_{TASK-1} led to prolongation of APD and an increase in plateau voltage (blue). A 2-fold increased I_{TASK-1} current shortened APD and decreased plateau voltage (red). (B), Net membrane currents with (black) and without (blue) I_{TASK-1}. (C), L-type calcium current (I_{CaL}) with (black) and without (blue) I_{TASK-1}. (D-F), The effects of I_{TASK-1} subtraction on other currents. (D), Effects on I_{Kur} (black/blue). (E), Effects on I_{Kr} (black/grey) and I_{Ks} (green/blue). (F), Effects on the inward rectifier current (I_{K1}) (black/blue).

of TASK-1 is able to make a significant contribution to the shortening of the action potential which was previously described for electrical remodeling in AF [2].

Development of a Markov model of TASK-1 channels

After preparation of atrial cardiomyocytes by enzymatic digestion, we and others have observed depolarized membrane potentials of about -60 mV. Thus, to record action potentials from single atrial cardiomyocytes with patch clamp and dynamic patch clamp recordings, we hyperpolarized the cells with a negative offset current injection. This current offset however, might interfere with the shape and duration of the action potentials we recorded. Thus, to further test our hypothesis that TASK-1 block can prolong atrial action potential duration, we investigated the role of TASK-1 using a computer model of atrial action potentials, described previously by Courtemanche et al. [13]. As a first step in the characterization of the role of TASK-1 *in silico*, we developed a Markov model of TASK-1 channel gating. For this purpose we analyzed the currents carried by TASK-1 channels expressed in *Xenopus* oocytes (Fig. 4). First, we recorded current voltage relationships (Fig. 4A, B) of TASK-1 and analyzed the kinetics of activation (Fig. 4C, D) and the fraction of quasi-instantaneous currents (Fig. 4E). The activation of I_{TASK-1} was well described with a bi-exponential fit. The two time constants of activation and the respective amplitudes are given in Fig. 4C and D. The instantaneous current (Fig. 4E) was estimated by back-extrapolation of the bi-exponential fit to the start of the test pulse. Next, we recorded the kinetics of deactivation (Fig. 4F) and the fraction of current that actually displayed deactivation kinetics (Fig. 4F, G).

The deactivating currents were sufficiently described by a mono-exponential fit and the time constants for the different potentials are given in Fig. 4H. The data of the TEVC recordings were subsequently used to derive a three state gating model of TASK-1 (Fig. 4I). The rate coefficients are given in Table 3 (see also Methods section for equations). This Markov model was able to reproduce the whole cell current kinetics recorded with the TEVC technique (Fig. 4B-E, G-H). We simulated TASK-1 whole cell currents (Fig. 4I) using the same voltage protocols as in the TEVC recordings (Fig. 4A, F). Simulated currents closely resemble the measured currents (Fig. 4A, F versus Fig. 4I). Thus, we conclude that the three state Markov model adequately describes major features of TASK-1 currents.

Action potential modeling confirms the role of I_{TASK-1} in human atrial cardiomyocytes

We then used the three state Markov model of TASK-1 for computational studies of human atrial action potentials. We applied the mathematical model of Courtemanche *et al.* which gives a comprehensive description of the electrophysiological behaviour of human atrial cardiomyocytes [13]. The calculated I_{TASK-1} was subtracted from the total transmembrane current to simulate a block of TASK-1 (Fig. 5A). Alternatively, we doubled I_{TASK-1} to simulate a transcriptional up-regulation of TASK-1 under AF (Fig. 5A). Simulated action potentials and the underlying currents are presented in Fig. 5. APD_{50} and APD_{90} of atrial cells paced at 1 Hz were 214.7 ms and 319.1 ms, respectively. After subtraction of I_{TASK-1} the APD_{50} was prolonged to 251.3 ms (+17 %) and the APD_{90} was prolonged to 357.2 ms (+12 %). Doubling of I_{TASK-1} in the cell model resulted in significant shortening of the atrial action potential, with an APD_{50} of 180.8 ms (-16 %) and an APD_{90} of 276.1 ms (-13 %). Thus, our computational study supports the observation from our patch clamp studies that I_{TASK-1} influences atrial action potential duration.

When TASK-1 was subtracted from the membrane currents to mimic TASK-1 block, we observed several changes in cellular electrophysiology (Fig. 5B-F). First, the net transmembrane current was altered (Fig. 5B, blue line). The minimal net outward current during the plateau phase of the action potential was further reduced (Fig. 5B, blue line), resulting even in a brief net inward current (blue line, arrow). Consistent with a net inward current, our calculations predict a more pronounced and prolonged Ca^{2+} influx via L-type Ca^{2+} channels (Fig. 5C). After block of I_{TASK-1}, a prolonged I_{Kur} efflux was calculated, which was probably related to the prolongation of the action potential (Fig. 5D). Interestingly, I_{Kr} and I_{Ks} are also expected to be increased in response to the block of I_{TASK-1} (Fig. 5E). Due to the prolongation of the action potential, the repolarizing I_{K1} increase occurred with a delay (Fig. 5F).

We conclude from our action potential modeling that an increase or a decrease in I_{TASK-1} can significantly alter action potential shape and duration in human atrial myocytes.

Discussion

Alteration of cardiac repolarization is considered to be one of the major causes of atrial fibrillation [20], and pharmacological modulation of atrial ion channels has been suggested as a useful approach for treating atrial fibrillation [21]. At present, pharmacological therapy of atrial arrhythmias is far from satisfactory. Besides low effectiveness in converting patients with chronic AF to sinus rhythm and in maintaining normal sinus rhythm [22], the drugs currently available lack specificity and/or cause adverse effects [23]. The most prominent side effect or complication is the drug-induced LQT syndrome, mostly caused by block of cardiac hERG channels [24]. In order to avoid this life-threatening complication, research on novel pharmacological therapies focuses on drug targets with atrium specific expression. Therefore, the GIRK channels which encode the sino-atrial I_{KACh} and the ion channels contributing to atrial I_{Kur} are promising proteins to target AF [23].

Kv1.5 channels are the major constituents of both rat [25, 26] and human [27-29] I_{Kur}. In rat, Kv1.5 contributes to ventricular I_{Kur} [25, 26], whereas in humans the I_{Kur} density is large in the atria but small or absent in the ventricle [30]. It is also noteworthy that I_{Kur} in human cardiac tissue might differ from that of the commonly studied animals such as the rat or guinea pig. Thus, to identify novel atrium-specific potassium channels and to identify novel drug targets against AF, it is crucial to determine the ion channel expression pattern in native human atrial cardiomyocytes and to measure the corresponding currents [31]. In the present study, we have analyzed the expression pattern of TASK-1 channels in the human heart and have functionally characterized TASK-1 channels in human atrial cardiomyocytes. Similar to the Kv1.5 channel, which is currently one of the most promising ion channel drug targets for AF [23], the expression of TASK-1 in human heart is restricted to

supraventricular regions. We have shown the presence of TASK-1 channels in right human atrial auricles by single channel recordings and have quantified the whole cell TASK-1 current in right human atrial auricles using the novel TASK blocker A293 [6]. The current density of I_{TASK-1} (0.38 pA/pF) in human atrial auricles is in the same range as previously described in rat and mouse ventricular cardiomyocytes [6, 7].

We found that I_{TASK-1} contributes up to 15 % to the sustained potassium current (I_{Ksus}) in human right auricles and comprises about 28 % of the background current in human atrial myocytes.

Although I_{TASK-1} in human atrial cardiomyocytes has only a relatively small current density the channels can modulate action potential duration. This notion is based on our findings that in mouse and rat ventricular cardiomyocytes TASK-1 currents with a similar magnitude can modulate action potential duration [6, 7]. Despite the large I_{to} currents present in rodent ventricular myocytes, we found that block or mathematical subtraction of a TASK-1 current of 0.4 pA/pF led to a prolongation of the rat ventricular action potential [6]. TASK-1 knock-out mice also show an increased action potential duration, as has been shown by our group [7] and by Donner et al. [32] using *in vivo* electrophysiological recordings [7] and surface electrocardiograms [7, 32]. We therefore conclude that although the amplitude of the TASK-1 currents in human atrial cells is small in comparison to that of other currents, TASK-1 can modulate human atrial action potential duration.

Our quantitative PCR data show that TASK-1 is strongly expressed in the human atrio-ventricular node as well. In addition, *in situ* hybridization experiments showed a high expression of TASK-1 mRNA in human sino-atrial node [33]. Although TASK-1 is expressed in mouse ventricular cardiomyocytes, the channel is predominantly expressed in the conduction system of the murine heart [34]. The high expression levels of TASK-1 channels in these cells suggest that I_{TASK-1} may also play a role in pacemaking and conduction. We found that hearts of TASK-1 knock-out mice have altered conduction properties, including for example a prolonged QRS complex in the surface electrocardiogram [7]. At present it is not clear whether block of I_{TASK-1} in human pacemaker cells or in cells of the conduction system might offer an additional benefit in the treatment of atrial arrhythmias or not.

There is evidence that TASK-1 expression may be altered in AF [17, 34]. However, altered TASK-1 expression in AF is still under debate. In 2005, Barth et al. found an up-regulation of TASK-1 transcripts in patients with AF [19]. In contrast, the group of Gaborit *et al.* reported that there is no change in TASK-1 expression in patients with chronic AF [35]. Our dynamic patch clamp recordings and our action potential modeling data indicate that increased TASK-1 currents can alter the shape and the duration of action potentials in human atrial cells. Thus, transcriptional up-regulation might contribute to the action potential shortening previously described as a part of the electrical remodeling during AF [2]. Interestingly, while Kv1.5 channels have been mostly reported to undergo down-regulation during AF [2, 17], TASK-1 was found to be transcriptionally up-regulated [19]. An increased expression of TASK-1 during AF raises the likelihood that pharmacological block of I_{TASK-1} may prolong the duration and change the shape of the human atrial action potential. It would be interesting to study the role of TASK-1 in patients suffering from atrial fibrillation. As there are no specific antibodies presently available for studying changes in TASK-1 protein levels, the TASK-1 blockers which we have reported [6, 36] might provide valuable tools for future studies probing altered TASK-1 channel expression at the plasma membrane.

It is not clear whether altered TASK-1 expression contributes to the genesis of AF. Nevertheless, the following findings support the idea that TASK-1 is a promising drug target for the treatment or prevention of this disease: (1) In human heart, TASK-1 expression is restricted to the atria, auricles and atrio-ventricular node, which allows selective modulation of atrial K^+ currents without affecting the electrical activity of the ventricles. (2) Up to 15 % of the atrial I_{Ksus} might be carried by I_{TASK-1} under normal conditions. (3) Block of I_{TASK-1} prolongs atrial action potential duration, as shown by our patch clamp experiments and by action potential modeling. (4) The mRNA levels of TASK-1 might be increased in patients with AF [19].

In conclusion, our data suggest that I_{TASK-1} might modulate action potential duration of human atrial cardiomyocytes. The lack of TASK-1 expression in human ventricles might raise the possibility to prolong atrial refractory period without causing ventricular side effects. Thus, block of atrial TASK-1 channels might be beneficial for the treatment or prevention of AF.

Acknowledgements

We thank Kirsten Ramlow for excellent technical support. We thank Heinz Köster, Sebastian Vogt, Alessandro Vannuchi, Lezek Piotr Rybinski, Stefan Waldhans and Ivo Martinovic for taking biopsy of atrial tissue. The compounds A293 and HMR1556 were obtained by Sanofi Aventis GmbH Germany. This work was supported by the Deutsche Forschungsgemeinschaft (DE-1482/2-1 to ND, DE-1482/3-1 to ND and JD and DE-1482/3-2 to ND). The computational studies were supported by the Richard A. and Nora Eccles Fund for Cardiovascular Research, and the Nora Eccles Treadwell Foundation.

References

1 Chugh SS, Blackshear JL, Shen WK, Hammill SC, Gersh BJ: Epidemiology and natural history of atrial fibrillation: clinical implications. J Am Coll Cardiol 2001;37:371-378.

2 Nattel S, Maguy A, Le Bouter S, Yeh YH: Arrhythmogenic ion-channel remodeling in the heart: heart failure, myocardial infarction, and atrial fibrillation. Physiol Rev 2007;87:425-456.

3 Ehrlich JR, Nattel S: Atrial-selective pharmacological therapy for atrial fibrillation: hype or hope? Curr Opin Cardiol 2009;24:50-55.

4 Nerbonne JM, Kass RS: Molecular physiology of cardiac repolarization. Physiol Rev 2005;85:1205-1253.

5 Goldstein SA, Bockenhauer D, O'Kelly I, Zilberberg N: Potassium leak channels and the KCNK family of two-P-domain subunits. Nat Rev Neurosci 2001;2:175-184.

6 Putzke C, Wemhöner K, Sachse FB, Rinné S, Schlichthörl G, Li XT, Jae L, Eckhardt I, Wischmeyer E, Wulf H, Preisig-Müller R, Daut J, Decher N: The acid-sensitive potassium channel TASK-1 in rat cardiac muscle. Cardiovasc Res 2007;75:59-68.

7 Decher N, Wemhöner K, Rinné S, Netter MF, Zuzarte M, Aller MI, Kaufmann SG, Li XT, Meuth SG, Daut J, Sachse FB, Maier SK: Knock-out of the potassium channel TASK-1 leads to a prolonged QT interval and a disturbed QRS complex. Cell Physiol Biochem 2011;28:77-86.

8 Bustamante JO, Watanabe T, Murphy DA, McDonald TF: Isolation of single atrial and ventricular cells from the human heart. Can Med Assoc J 1982;126:791-793.

9 Maier S, Aulbach F, Simm A, Lange V, Langenfeld H, Behre H, Kersting U, Walter U, Kirstein M: Stimulation of L-type Ca^{2+} current in human atrial myocytes by insulin. Cardiovasc Res 1999;44:390-397.

10 Decher N, Kumar P, Gonzalez T, Renigunta V, Sanguinetti MC: Structural basis for competition between drug binding and Kvbeta 1.3 accessory subunit-induced N-type inactivation of Kv1.5 channels. Mol Pharmacol 2005;68:995-1005.

11 Duprat F, Lesage F, Fink M, Reyes R, Heurteaux C, Lazdunski M: TASK, a human background K^+ channel to sense external pH variations near physiological pH. EMBO J 1997;16:5464-5471.

12 Abbruzzese J, Sachse FB, Tristani-Firouzi M, Sanguinetti MC: Modification of hERG1 channel gating by Cd^{2+}. J Gen Physiol 2010;136:203-224.

13 Courtemanche M, Ramirez RJ, Nattel S: Ionic mechanisms underlying human atrial action potential properties: insights from a mathematical model. Am J Physiol 1998;275:H301-321.

14 Press WH, Teukolsky SA, Vetterling WT, Flannery BP: *Numerical Recipes in C*. 2 ed. Cambridge: Cambridge University Press; 1992.

15 Musset B, Meuth SG, Liu GX, Derst C, Wegner S, Pape HC, Budde T, Preisig-Müller R, Daut J: Effects of divalent cations and spermine on the K^+ channel TASK-3 and on the outward current in thalamic neurons. J Physiol 2006;572:639-657.

16 Kim Y, Bang H, Kim D: TBAK-1 and TASK-1, two-pore K^+channel subunits: kinetic properties and expression in rat heart. Am J Physiol 1999;277:H1669-1678.

17 Van Wagoner DR, Pond AL, McCarthy PM, Trimmer JS, Nerbonne JM: Outward K^+ current densities and Kv1.5 expression are reduced in chronic human atrial fibrillation. Circ Res 1997;80:772-781.

18 Wettwer E, Hala O, Christ T, Heubach JF, Dobrev D, Knaut M, Varro A, Ravens U: Role of I_{Kur} in controlling action potential shape and contractility in the human atrium: influence of chronic atrial fibrillation. Circulation 2004;110:2299-2306.

19 Barth AS, Merk S, Arnoldi E, Zwermann L, Kloos P, Gebauer M, Steinmeyer K, Bleich M, Kääb S, Hinterseer M, Kartmann H, Kreuzer E, Dugas M, Steinbeck G, Näbauer M: Reprogramming of the human atrial transcriptome in permanent atrial fibrillation: expression of a ventricular-like genomic signature. Circ Res 2005;96:1022-1029.

20 Michael G, Xiao L, Qi XY, Dobrev D, Nattel S: Remodelling of cardiac repolarization: how homeostatic responses can lead to arrhythmogenesis. Cardiovasc Res 2009;81:491-499.

21 Nattel S, Carlsson L: Innovative approaches to anti-arrhythmic drug therapy. Nat Rev Drug Discov 2006;5:1034-1049.

22 Burashnikov A, Antzelevitch C: New developments in atrial antiarrhythmic drug therapy. Nat Rev Cardiol 2010;7:139-148.

23 McBride BF: The emerging role of antiarrhythmic compounds with atrial selectivity in the management of atrial fibrillation. J Clin Pharmacol 2009;49:258-267.
24 Mitcheson JS, Chen J, Lin M, Culberson C, Sanguinetti MC: A structural basis for drug-induced long QT syndrome. Proc Natl Acad Sci U S A 2000;97:12329-12333.
25 Dixon JE, McKinnon D: Quantitative analysis of potassium channel mRNA expression in atrial and ventricular muscle of rats. Circ Res 1994;75:252-260.
26 Guo W, Kamiya K, Toyama J: Roles of the voltage-gated K^+ channel subunits, Kv1.5 and Kv1.4, in the developmental changes of K^+ currents in cultured neonatal rat ventricular cells. Pflügers Arch 1997;434:206-208.
27 Wang Z, Fermini B, Nattel S: Sustained depolarization-induced outward current in human atrial myocytes. Evidence for a novel delayed rectifier K^+ current similar to Kv1.5 cloned channel currents. Circ Res 1993;73:1061-1076.
28 Fedida D, Wible B, Wang Z, Fermini B, Faust F, Nattel S, Brown AM: Identity of a novel delayed rectifier current from human heart with a cloned K^+ channel current. Circ Res 1993;73:210-216.
29 Snyders DJ, Tamkun MM, Bennett PB: A rapidly activating and slowly inactivating potassium channel cloned from human heart. Functional analysis after stable mammalian cell culture expression. J Gen Physiol 1993;101:513-543.
30 Nerbonne JM: Molecular basis of functional voltage-gated K^+ channel diversity in the mammalian myocardium. J Physiol 2000;525:285-298.
31 Nattel S, Frelin Y, Gaborit N, Louault C, Demolombe S: Ion-channel mRNA-expression profiling: Insights into cardiac remodeling and arrhythmic substrates. J Mol Cell Cardiol 2010;48:96-105.
32 Donner BC, Schullenberg M, Geduldig N, Huning A, Mersmann J, Zacharowski K, Kovacevic A, Decking U, Aller MI, Schmidt KG: Functional role of TASK-1 in the heart: studies in TASK-1-deficient mice show prolonged cardiac repolarization and reduced heart rate variability. Basic Res Cardiol 2011;106:75-87.
33 Chandler NJ, Greener ID, Tellez JO, Inada S, Musa H, Molenaar P, Difrancesco D, Baruscotti M, Longhi R, Anderson RH, Billeter R, Sharma V, Sigg DC, Boyett MR, Dobrzynski H: Molecular architecture of the human sinus node: insights into the function of the cardiac pacemaker. Circulation 2009;119:1562-1575.
34 Graham V, Zhang H, Willis S, Creazzo TL: Expression of a two-pore domain K^+ channel (TASK-1) in developing avian and mouse ventricular conduction systems. Dev Dyn 2006;235:143-151.
35 Gaborit N, Steenman M, Lamirault G, Le Meur N, Le Bouter S, Lande G, Leger J, Charpentier F, Christ T, Dobrev D, Escande D, Nattel S, Demolombe S: Human atrial ion channel and transporter subunit gene-expression remodeling associated with valvular heart disease and atrial fibrillation. Circulation 2005;112:471-481.
36 Streit AK, Netter MF, Kempf F, Walecki M, Rinné S, Bollepalli MK, Preisig-Müller R, Renigunta V, Daut J, Baukrowitz T, Sansom M, Stansfeld PJ, Decher N: A specific two-pore-domain potassium channel blocker defines the structure of the TASK-1 open pore. J. Biol. Chem. 2011;286:13977-13984.
37 Wilders R: Dynamic clamp: a powerful tool in cardiac electrophysiology. J Physiol 2006;576:349-359.